

# INTERPOLATION AND THE CHIRP TRANSFORM: DSP MEETS OPTICS

*David C. Munson, Jr.*

Dept. Electrical and Computer Engineering  
and Coordinated Science Laboratory  
University of Illinois at Urbana–Champaign  
Urbana, IL 61801 USA

*Orhan Arikan*

Electrical and Electronics Engr. Dept.  
Bilkent University  
Bilkent 06533 Ankara, Turkey

## ABSTRACT

This paper considers the problem of interpolating a signal from one uniformly-spaced grid to another, where the grid spacings may be related by an arbitrary, irrational factor. Noting that interpolation is the digital equivalent of magnification, we begin by reviewing optical systems for magnification and “computation” of the chirp Fourier transform. This route suggests several analog schemes for magnification, which can be discretized to produce algorithms for interpolation. We then derive one of these algorithms from first principles, using a digital-signal-processing perspective. The result is an important, but forgotten, algorithm for interpolation first suggested as an application of the chirp-z transform by Rabiner, Schafer, and Rader. Unlike the earlier derivation, our approach is direct – we do not make use of Bluestein’s trick of completing the square. In addition, our approach identifies parameters under user control that can be optimized for best performance.

## 1. INTRODUCTION

Interpolation between two uniform grids is a requirement in many diverse fields including digital communications, image processing, and computational imaging. Displaying a part of an image at an increased size (zooming) requires accurate two-dimensional interpolation from one Cartesian grid to another by almost arbitrary factors. CT, MRI, and SAR are examples of computational imaging systems that require extensive interpolation.

Efficient and well known methods are available for sampling rate change from one uniform grid to another when the ratio of sampling periods,  $R$ , is a rational number with small factors [1, 2]. However, when  $R$  is irrational or a ratio of two large primes, it is widely believed that  $R$  must be rounded to a rational  $\hat{R}$  with small factors. Doing so causes error. Another problem with some interpolation approaches is the required design of exceedingly high-order FIR filters. Due to these difficulties, other methods of sampling rate change have been proposed [3]. These methods are based on the idea of employing non-periodically shift-varying FIR filters instead of the periodically shift-varying structure of earlier methods [4]. However, these methods require either a huge memory to store the filter coefficients, or a considerable amount of computation to update the filter coefficients between every two consecutive outputs [3].

An exception is an algorithm utilizing the chirp transform, which was revealed many years ago [5]<sup>1</sup>. In this important work,

---

<sup>1</sup>In this paper we have use for the chirp-z transform evaluated only on the unit circle in the z-plane (not on a contour that spirals inward or

the operation of interpolation was briefly considered as an application of the chirp transform, and then forgotten. Indeed, several years ago, we rediscovered the method of “chirp interpolation” and published a comprehensive study of this technique [7, 8]. A number of applications use chirp interpolation, including the linogram method in tomography [9, 10] and the chirp scaling image formation algorithm in strip-mapping SAR [11]. More fundamentally, the mathematical basis of chirp interpolation has been known for many years in the optics community where magnification is the analog version of interpolation [12, 13].

This paper has two thrusts. We begin in Section 2 by reviewing simple optical systems for magnification and “computation” of the Fourier transform. We show analog signal processing equivalents of these systems involving multiplications by and convolutions with linear FM chirp signals. These notions form the conceptual basis for several approaches to interpolation by an arbitrary factor. The second thrust is to then devise an efficient digital scheme for implementing one of the interpolators suggested by the optical analysis. Instead of attempting a direct discretization, Sections 3 and 4 present a “DSP approach” to arriving at the same point, which was originally presented in [7, 8]. Section 3 provides the Fourier-domain relation between the original and the interpolated sequences. Then, using this analysis and making a number of approximations, Section 4 gives a derivation of a chirp interpolation algorithm that corresponds to one of the systems suggested by the optical analogy. Unlike the original derivation in [5], our approach is direct – we do not make use Bluestein’s trick of completing the square. As a biproduct of our approach, we identify parameters in the chirp interpolation algorithm that can be optimized for best performance. We also show how block processing can be used to interpolate sequences of arbitrary length.

## 2. OPTICAL CONCEPTS UNDERLYING INTERPOLATION AND THE CHIRP TRANSFORM

Magnification in an optical system is the analog equivalent to interpolation. Figure 1 (a) shows the geometry for a simple optical magnification system [12]. We assume a monochromatic coherent wave propagating in a direction along the axis of the lens. For simplicity, we restrict to a 1-D version of this system where  $g(x)$  is the complex amplitude of the wavefront in the input plane at distance  $d_1$  from the lens. Here,  $x$  represents the vertical spatial coordinate. If we define the output plane to be at distance  $d_2$  from the lens and

---

outward). In keeping with the modern terminology employed in [6], we refer to this special and most important case of the chirp-z transform as the chirp transform.

select  $d_1$  and  $d_2$  so that they satisfy the lens law

$$1/d_1 + 1/d_2 = 1/f \quad (2.1)$$

where  $f$  is the focal length of the lens, then the complex amplitude of the field in the output plane will be a magnified (and inverted) version of  $g(x)$ , as given [12]. The signal processing equivalent to the optical magnification system is shown in Figure 1 (b). Here, we have used the fact that the Fresnel approximation to propagation corresponds to convolution with a linear FM signal, and that a lens imparts quadratic phase. Thus, the two boxes in Figure 1 (b) are linear shift-invariant systems with the chirp impulse responses shown, and the multiplication by a chirp signal models the lens. This system is the same as that on p. 203 in [13], except that we have shown the exact output described at the top of p. 204. This system can be modified to create the system in Figure 1 (c), which produces a noninverted output without the multiplicative phase term.

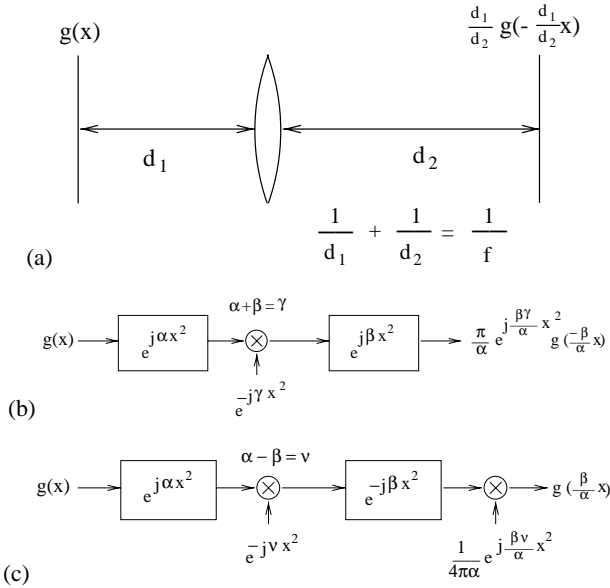


Figure 1: (a) Optical magnification system. (b) Corresponding signal processing system that produces essentially the same result. (c) System that produces a noninverted output.

Discretizing Figure 1(c) will lead to an algorithm for interpolation by arbitrary factors. However a larger class of approaches to interpolation can be motivated by considering first a lens with the standard Fourier transform geometry shown in Figure 2(a) where both the input and output planes are located a focal distance from the lens [12]. The corresponding analog signal processing system is shown in Figure 2 (b). (It requires some tricky algebra to show that this system produces the output shown.) This system can be simplified to a system containing two multipliers and a single filtering operation, which is shown in Figure 3 (a), and which is equivalent to the system shown on p. 201 in [13].

Both Figures 2 (b) and 3 (a) produce frequency-scaled versions of the Fourier transform, i.e., an analog chirp transform. However, in this paper we shall reserve the term chirp Fourier transform for only Figure 3 (a), which is the continuous-time version of the digital chirp transform on p. 625 in [6]. Figure 3 (b) shows an analog inverse chirp Fourier transform. Now, since a

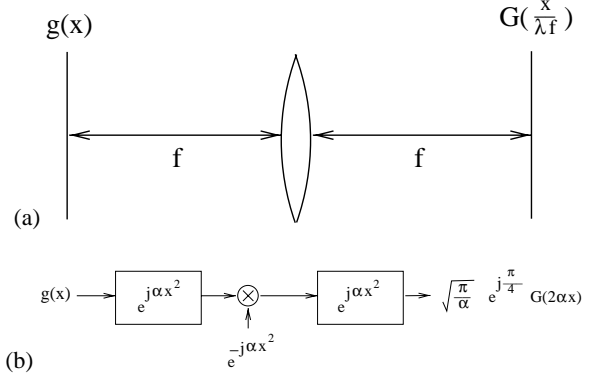


Figure 2: (a) Optical Fourier transform system. (b) Corresponding signal processing system that produces a similar result.

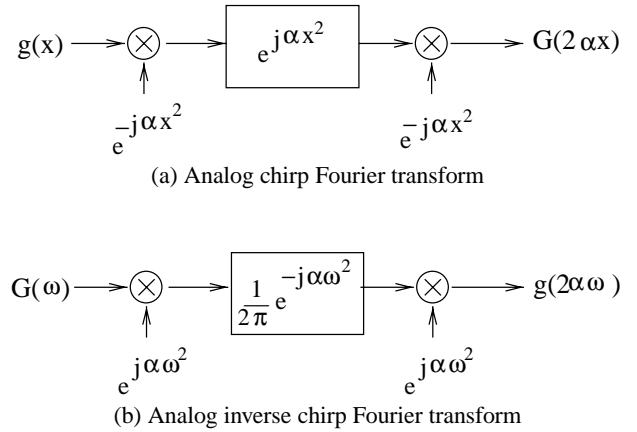


Figure 3: Schemes for computing scaled forward and inverse Fourier transforms.

scaled Fourier transform corresponds to a scaled (inversely) time or spatial-domain function, there are many ways to combine forward and inverse Fourier and chirp Fourier transforms to produce interpolators. Three of these schemes are shown in Figure 4. Figure 4 (c) splits the magnification between two chirp Fourier transforms. In the next two sections we derive a discrete form of Figure 4 (a), which is the chirp interpolation algorithm first mentioned in [5]. In a similar way, we could derive a discrete version of Figure 4(b). Our approach is considerably different from that in [5, 6], which relies on the Bluestein trick of completing the square. We instead base our derivation on how the alteration of the sampling rate in the time domain affects the scaling of the Fourier variable in the discrete-time Fourier transform.

### 3. FOURIER-DOMAIN RELATION BETWEEN ORIGINAL AND INTERPOLATED SEQUENCES

In this section, we develop the Fourier-domain relation between samples of a bandlimited analog signal taken at two different rates. Let  $x_1(n)$  and  $x_2(n)$  be samples of an analog signal  $x_a(t)$  taken at uniform intervals of  $T_1$  and  $T_2$ , respectively. The Discrete-Time Fourier Transforms (DTFTs) of the sample sequences are defined

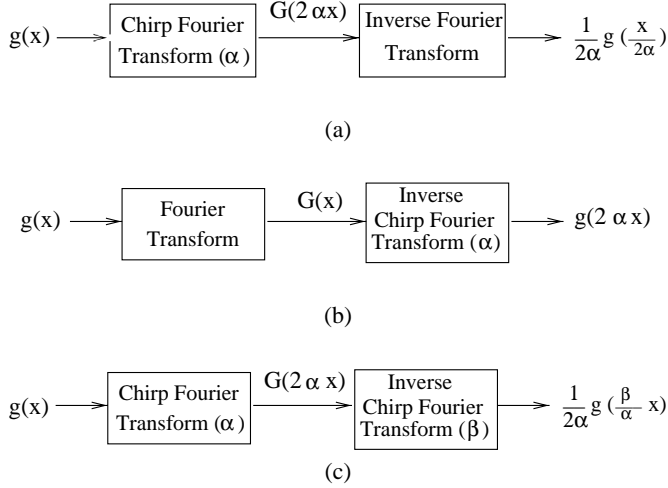


Figure 4: Schemes for magnification (interpolation) by an arbitrary factor. Chirp Fourier Transform refers to Figure 3(a). Inverse Chirp Fourier Transform refers to Figure 3(b).

as usual by

$$X_i(\lambda) = \sum_{n=-\infty}^{\infty} x_i(n)e^{-jn\lambda} \quad (3.2)$$

Our goal is to express  $X_2(\lambda)$  in terms of  $X_1(\lambda)$ . This will lead us to the chirp interpolation algorithm suggested by Figure 4(a).

Assuming  $T_1$  satisfies the Nyquist criterion, the Fourier transform of  $x_a(t)$ ,  $X_a(\omega)$ , is related to the DTFT of  $x_1(n)$  by

$$X_a(\omega) = \begin{cases} T_1 X_1(T_1 \omega), & |\omega| \leq \frac{\pi}{T_1}, \\ 0, & \frac{\pi}{T_1} < |\omega|, \end{cases} \quad (3.3)$$

Similarly, if  $T_2$  also meets the Nyquist criterion, we can write

$$X_2(\lambda) = \frac{1}{T_2} X_a\left(\frac{\lambda}{T_2}\right), \quad |\lambda| \leq \pi. \quad (3.4)$$

Both 3.3 and 3.4 follow from the standard relation

$$X_i(\lambda) = \frac{1}{T_i} \sum_{k=-\infty}^{\infty} X_a\left(\frac{\lambda + 2\pi k}{T_2}\right) \quad (3.5)$$

where the terms of the summation do not overlap if the sampling period satisfies the Nyquist criterion. Now, if  $T_2 < T_1$  which corresponds to an increase in sampling rate, by using 3.3 and 3.4, we can express  $X_2(\lambda)$  in terms of  $X_1(\lambda)$  as

$$X_2(\lambda) = \begin{cases} \frac{T_1}{T_2} X_1\left(\frac{T_1}{T_2} \lambda\right), & |\lambda| \leq \frac{T_2}{T_1} \pi, \\ 0, & \frac{T_2}{T_1} \pi < |\lambda| \leq \pi, \end{cases} \quad (3.6)$$

Alternatively, if  $T_2 \geq T_1$ , corresponding to a decrease in sampling rate, we have

$$X_2(\lambda) = \frac{T_1}{T_2} X_1\left(\frac{T_1}{T_2} \lambda\right), \quad |\lambda| \leq \pi. \quad (3.7)$$

By using the above relationship and the inverse DTFT, we can express  $x_2(n)$  as

$$x_2(n) = \frac{1}{2\pi} \int_{-\Lambda}^{\Lambda} \frac{T_1}{T_2} \left( \sum_{m=-\infty}^{\infty} x_1(m) e^{-j\frac{T_1}{T_2} m \lambda} \right) e^{jn\lambda} d\lambda, \quad (3.8)$$

where the integration limit is defined as:

$$\Lambda = \min\left(\frac{T_2}{T_1} \pi, \pi\right). \quad (3.9)$$

Equation 3.8 explicitly relates the two sample sequences to each other. However, the infinite summation in 3.8 makes it impractical to directly use 3.8 to obtain  $x_2(n)$  from  $x_1(n)$ . Therefore, we will use the following approximate relationship where the infinite summation is truncated and the integration is approximated by its uniform Riemann approximation

$$x_2(n) \simeq \frac{\Delta}{2\pi} \frac{T_1}{T_2} \sum_{k=-\frac{L}{2}}^{\frac{L}{2}-1} \sum_{m=-\frac{N_1}{2}}^{\frac{N_1}{2}-1} x_1(m) w(m) e^{-j\Delta k \left(\frac{T_1}{T_2} m - n\right)} \alpha(k), \quad (3.10)$$

where  $\alpha$  is a weighting function that can be applied to the Riemann sum which uses uniform intervals of size  $\Delta$  and  $L = \frac{2\Lambda}{\Delta}$ . Here it is assumed that both  $N$  and  $L$  are chosen as even numbers. To avoid potential frequency aliasing, for all  $m$  and  $n$  the choice of  $\Delta$  must satisfy

$$\left| \Delta \left( \frac{T_1}{T_2} m - n \right) \right| \leq \pi \quad (3.11)$$

which is assured by choosing  $\Delta$  as

$$\Delta = \frac{2\pi}{M}, \text{ for } M \geq \frac{T_1}{T_2} N_1 + N_2. \quad (3.12)$$

In the following section, we derive the steps of the chirp interpolation algorithm which efficiently computes 3.10. Before going into details of the algorithm, however, we first simulate 3.10 to show that it produces an accurate interpolation. In our simulation we suppose that the input sequence  $x_1(n)$  is 182 Nyquist rate samples of an analog signal that is bandlimited to  $\pi$  rad/sec. ( $T_1 = 1$ ), and that we are required to obtain  $x_2(n)$  which are samples of the analog signal obtained at a rate  $\sqrt{2}$ , which represents a change in sampling rate by an irrational factor. The original analog signal is chosen to be:

$$x_a(t) = \sum_{k=1}^{100} a_k \frac{\sin(2\pi f_k(t - t_k))}{2\pi f_k(t - t_k)} \quad (3.13)$$

where  $a_k$ ,  $f_k$  and  $t_k$  are uniform random variables on the intervals  $[-1, 1]$ ,  $[0, 0.5]$  and  $[-\frac{N_1 T_1}{2}, \frac{N_1 T_1}{2}]$  respectively. The output samples  $x_2(n)$  were approximated by using 3.10 where  $\Delta$  was chosen as  $2\pi/512$ , and both weighting functions  $w(m)$  and  $\alpha(i)$  were chosen as 1 over their respective regions of support: the integers in  $[-92, 91]$  and  $[-181, 181]$ . For this case, after a little algebra, 3.10 can be expressed as

$$x_2(n) \simeq \sqrt{2} \sum_{m=-92}^{91} x_1(m) \frac{1}{512} \frac{\sin\left(\frac{362\pi(\sqrt{2}m-n)}{512}\right)}{\sin\left(\frac{\pi(\sqrt{2}m-n)}{512}\right)}, \quad (3.14)$$

which is a close approximation to Shannon sinc interpolation. This formula was used to compute interpolated samples  $\hat{x}_2(n)$  for  $-128 \leq n \leq 127$ . In Fig. 5, both the actual samples and the interpolation error is shown.

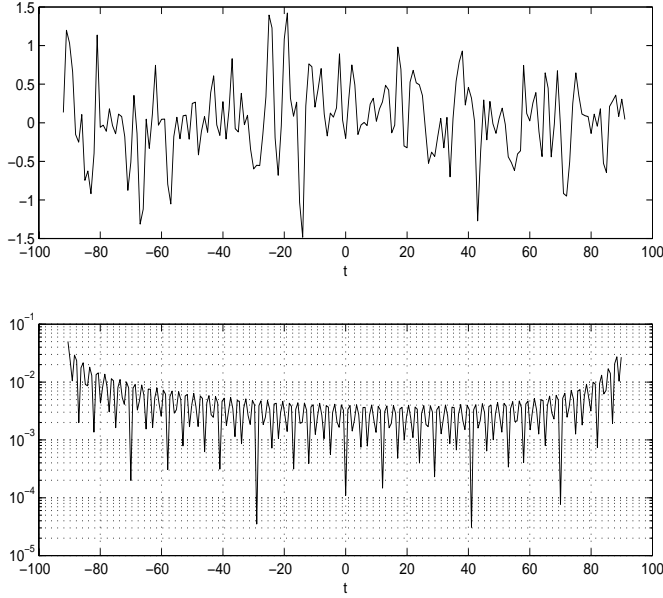


Figure 5: An example of chirp interpolation by a factor of  $\sqrt{2}$ : actual signal (top) and the magnitude of the interpolation error (bottom).

#### 4. CHIRP INTERPOLATION ALGORITHM

Direct computation of 3.10 requires  $O(N^2)$  complex multiplications when the number of input samples is  $N$ . Here we present an efficient method for computing 3.10 using the chirp transformation.

The required computation of 3.10 can be performed in two steps: first compute

$$h(k) = \sum_{m=-\frac{N_1}{2}}^{\frac{N_1}{2}-1} \left[ x_1(m) w(m) e^{-j\frac{T_1}{T_2} m^2 \frac{\Delta}{2}} \right] e^{j\frac{T_1}{T_2} (m-k)^2 \frac{\Delta}{2}}, \quad (4.15)$$

and then compute the approximate output samples  $\hat{x}_2(n)$  as

$$\hat{x}_2(n) = \frac{\Delta}{2\pi} \frac{T_1}{T_2} \sum_{k=-\frac{L}{2}}^{\frac{L}{2}-1} h(k) e^{-j\frac{T_1}{T_2} k^2 \frac{\Delta}{2}} \alpha(k) e^{jn k \Delta}. \quad (4.16)$$

The first step together with the multiplication of  $h(k)$  by the first complex exponential in 4.16, constitute a chirp transformation [5]. Here, we have moved the multiplication by this complex exponential into the second step for further computational saving. To see that these two steps are equivalent to 3.10, one can substitute 4.15 in 4.16. This form of computation is preferred to the Shannon sinc interpolation formula because the first step is a convolution, and with the choice of  $\Delta$  given in 3.12 the second step is an inverse DFT, both of which can be efficiently computed via the FFT. Both weighting sequences,  $w(m)$  and  $\alpha(k)$ , can be optimized for best performance. We will report on this in a future paper.

By making use of block processing, the chirp interpolation algorithm can also be used to process long input sequences. However, note that in the presentation of the chirp algorithm it was

assumed that the input and output samples were "lined up" at the origin, that is,  $x_2(0) = x_1(0)$ , which may not be valid in the processing of input blocks. Fortunately, this alignment problem can be overcome easily by applying the necessary shifts to both the input and the interpolated signals in the Fourier domain. Assuming that each input block has length  $N_1$  and each output block has length  $N_2$ , then to process the  $p^{\text{th}}$  input block to obtain the  $q^{\text{th}}$  output block the first step of the chirp algorithm given by 4.15 should be modified as:

$$h(k) = h(k) e^{j(qN_2 - pN_1 \frac{T_1}{T_2}) \Delta 2k}. \quad (4.17)$$

#### 5. ACKNOWLEDGMENT

The authors sincerely thank Nail Çadallı for his assistance in assembling this manuscript.

#### 6. REFERENCES

- [1] R. Schafer and L. Rabiner, "A digital signal processing approach to interpolation," *Proc. IEEE*, vol. 61, pp. 692-702, June 1973.
- [2] R. E. Crochiere and L. R. Rabiner, *Multirate Digital Signal Processing*. Englewood Cliffs, NJ: Prentice-Hall, 1983.
- [3] T. A. Ramstad, "Digital methods for conversion between arbitrary sampling frequencies," *IEEE Trans. Acoust., Speech, Signal Processing*, vol. 32, pp. 577-591, June 1984.
- [4] R. Ansari and B. Liu, "Interpolators and decimators as periodically time-varying filters," in *Proc. IEEE Int. Symp. Circuits and Systems*, 1981, pp. 447-450.
- [5] L. Rabiner, R. Schafer, and C. Rader, "The chirp-z transform and its applications," *Bell Syst. Tech. J.*, vol. 48, pp. 1249-1292, May 1969.
- [6] A. V. Oppenheim and R. W. Schaffer, *Discrete-Time Signal Processing*. Englewood Cliffs, NJ: Prentice-Hall, 1989.
- [7] O. Arkan, "Investigation of topics in radar signal processing," Ph.D. dissertation, University of Illinois, Urbana, IL, 1990.
- [8] O. Arkan and D. C. Munson, Jr., "Interpolation between two uniform grids with arbitrary spacings," *Proc. 1990 Bilkent Int. Conf. on New Trends in Communication, Control, Signal Processing*, Ankara, Turkey, pp. 1044-1058, July 2-5, 1990.
- [9] P. Edholm, G. Herman, and D. Roberts, "Image reconstruction from linograms: Implementation and evaluation," *IEEE Trans. Med. Imaging*, vol. 7, pp. 239-246, September 1988.
- [10] H. Choi and D. C. Munson, Jr., "Direct Fourier reconstruction in tomography and synthetic aperture radar," *Int. J. Imaging Systems and Technology*, vol. 9, pp. 1-13, Jan. 1998.
- [11] R. K. Raney, H. Runge, R. Bamler, I. Cumming, and F. Wong, "Precision SAR processing using chirp scaling," *IEEE Trans. Geoscience and Remote Sensing*, vol. 32, pp. 786-799, June 1994.
- [12] J. W. Goodman, *Introduction to Fourier Optics*. New York, NY: McGraw-Hill, 1968.
- [13] A. Papoulis, *Systems and Transforms with Applications in Optics*. New York, NY: McGraw-Hill, 1968.